Inorg. Chem. **2007**, *46*, 7782–7788

Mixed-Valence Iron(II, III) Trimesates with Open Frameworks Modulated by Solvents

Linhua Xie, Shuxia Liu,* Chaoying Gao, Ruige Cao, Jianfang Cao, Chunyan Sun, and Zhongmin Su

Key Laboratory of Polyoxometalates, Science of Ministry of Education, College of Chemistry, Northeast Normal University, Changchun City, JiLin, P. R. China 130024

Received November 30, 2006

Solvothermal reactions with different solvents produced two iron trimesates $[Fe_2(H_2O)_2(BTC)_{4/3}]Cl\cdot 4.5(DMF)$ (**1**) and $[Fe_4Cl(BTC)_{8/3}]Cl_2\cdot H_2O\cdot 2.5(DEF)$ (**2**) (BTC = 1,3,5-benzenetricarboxylate, DMF = *N*,*N*′-dimethylformamide, DEF = *N*,*N*′-diethylformamide). The framework of **1** is a (3,4)-connected net constructed from mixed-valence paddlewheel Fe_2(II, III) units and BTC linkers, while the framework of **2** is a (3,8)-connected net built from mixed-valence square-planar Fe_4(III, III, III, II) units and BTC linkers. The large volume inside the framework of **1** (or **2**) is occupied by disordered Cl^- anions and guest DMF (or DEF) molecules. The mixed-valence character of the frameworks of **1** and **2** was confirmed by Mössbauer spectroscopy studies. The active electronic property of iron cations may be the origin of the variability of the iron–organic frameworks, which are readily affected by some synthetic factors, such as solvents. Magnetic studies reveal that there are antiferromagnetic exchange interactions among the Fe atoms in **1** and **2**. Ion-exchange studies for **1** show that the Cl^- anions inside the framework of **1** can be exchanged by CNS^- anions.

Introduction

Iron ions play an essential part in biological systems due to their electron-transfer ability that is vital in metabolic processes in accompaniment with redox and catalysis. For instance, in hemerythrin,[1] there is a non-heme diiron cluster in its active site for the reversible bonding of dioxygen. The two ferrous cations bridged by two carboxylate groups and one hydroxide ion are respectively six- (Fe1) and five-coordinated (Fe2) with the other sites occupied by imidazole groups from histidine residues. (Figure 1) When O_2 is carried, the Fe2 atom of the cluster achieves saturated six-coordination and the O_2 molecule is picked up in the form of a hydroperoxide anion. The bridging hydroxide ion transforms into an oxo bridge with hydrogen bonding to the hydroperoxide anion. The two iron atoms turn to be trivalent by electrons transferred into the O_2 molecule.

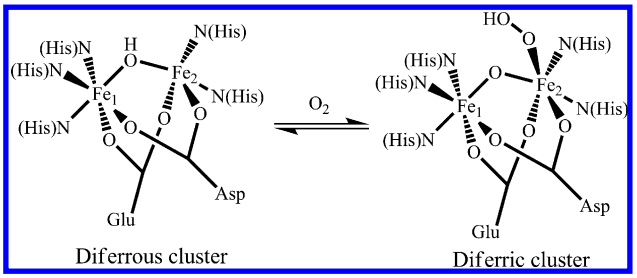

Figure 1. Schematic structures of the diiron cluster in hemerythrin before and after the uptake of dioxygen.

On the other hand, metal−organic frameworks[2−6] have been regarded as promising materials with many applications, especially in hydrogen storage[7,8] and catalysis.[9,10] For hydrogen storage, however, challenges still remain, for the dihydrogen can only be well physisorbed into the pores of

* To whom correspondence should be addressed. E-mail: liusx@nenu.edu.cn. Fax: +86-431-85099328.

(1) Du Bois, J.; Mizoguchi, T. J.; Lippard, S. J. *Coord. Chem. Rev.* **2000**, *200*, 443−485.
(2) Yaghi, O. M.; O'Keeffe, M.; Ockwig, N. W.; Chae, H. K.; Eddaoudi, M.; Kim, J. *Nature* **2003**, *423* (6941), 705−714.
(3) James, S. L. *Chem. Soc. Rev.* **2003**, *32* (5), 276−288.
(4) Kitagawa, S.; Kitaura, R.; Noro, S. *Angew. Chem., Int. Ed.* **2004**, *43* (18), 2334−2375.
(5) Rao, C. N. R.; Natarajan, S.; Vaidhyanathan, R. *Angew. Chem., Int. Ed.* **2004**, *43* (12), 1466−1496.
(6) Rowsell, J. L. C.; Yaghi, O. M. *Microporous Mesoporous Mater.* **2004**, *73* (1−2), 3−14.
(7) Férey, G.; Latroche, M.; Serre, C.; Millange, F.; Loiseau, T.; Percheron-Guégan, A. *Chem. Commun.* **2003** (*24*), 2976−2977.
(8) Rosi, N. L.; Eckert, J.; Eddaoudi, M.; Vodak, D. T.; Kim, J.; O'Keeffe, M.; Yaghi, O. M. *Science* **2003**, *300* (5622), 1127−1129.
(9) Seo, J. S.; Whang, D.; Lee, H.; Jun, S. I.; Oh, J.; Jeon, Y. J.; Kim, K. *Nature* **2000**, *404* (6781), 982−986.
(10) Dybtsev, D. N.; Nuzhdin, A. L.; Chun, H.; Bryliakov, K. P.; Talsi, E. P.; Fedin, V. P.; Kim, K. *Angew. Chem., Int. Ed.* **2006**, *45* (6), 916−920.

10.1021/ic062273m CCC: $37.00
Published on Web 08/15/2007

metal−organic frameworks at low temperature with overpressure required.[11] To overcome these barriers, increasing the adsorbate−adsorbent interactions is evidently crucial.[12] For the active electronic property as in biological systems, iron ions may serve as good active sites when incorporated into the walls of porous metal−organic frameworks, and especially if the metal centers are coordinatively unsaturated with open coordination sites. However, investigations of iron−organic frameworks are less common compared with those of zinc and copper, etc.[13−21] The main reason is that Fe^{2+} is air-sensitive and readily changes into Fe^{3+}, and Fe^{3+} has a strong tendency to undergo hydrolysis into a stable polymeric hydrous iron oxide even in a strongly acidic environment,[22,23] whereas alkalescency is favorable for the construction of frameworks with high dimensionalities. For example, deprotonation is required for carboxylic acid ligands.

With the above considerations in mind and motivated by our previous study of zinc 1,3,5-benzenetricarboxylate (BTC),[24] we investigated the iron−BTC system under solvothermal conditions. We isolated three-dimensional (3D) mixed-valence open frameworks $[Fe_2(H_2O)_2(BTC)_{4/3}]Cl\cdot 4.5(DMF)$ (**1**) (DMF = *N*,*N*′-dimethylformamide) and $[Fe_4Cl(BTC)_{8/3}]\text{-}Cl_2\cdot H_2O\cdot 2.5(DEF)$ (**2**) (DEF = *N*,*N*′-diethylformamide) with respective employment of the DMF and DEF solvents. The two-dimensional compound $[Fe_2Cl_2(HBTC)_2](HTEDA)_2$ (**3**) (TEDA = triethylenediamine) was the byproduct of the reaction for **2**. Herein, the syntheses and structures of the three compounds, magnetic properties, and results of host−guest studies for **1** and **2** are presented.

Experimental Section

Materials and General Methods. Solvents and reagents were obtained from commercial sources and used as received. Elemental analyses were performed on a PLASMA-SPEC(I) ICP atomic-emission spectrometer (Fe) and a Perkin-Elmer 240C elemental analyzer (C, H, N). IR spectra were recorded in the range of 400−4000 cm^{-1} on an Alpha Centaurt FT/IR spectrophotometer using KBr pellets. Thermal gravimetric (TG) analyses were performed on a Perkin-Elmer TGA7 instrument in flowing N_2 with a heating rate of 10 °C/min. Powder X-ray diffraction measurements were performed on a Rigaku D/MAX-3 instrument with Cu Kα radiation in the angular range $2\theta = 3-90°$at 293 K. The X-ray photoeletron spectrum (XPS) was recorded with a VG ESCALAB MK II Electron Spectrometer. Magnetic susceptibility data were collected over the temperature range of 2−300 K at a magnetic field of 1000 Oe on a Quantum Design MPMS-5 SQUID magnetometer. Mössbauer spectra were recorded by an Oxford MS-500 model constant-acceleration Mössbauer spectrometer with a 1024 multichannel analyzer. The velocity was calibrated by an α-Fe foil. The radiation source was $^{57}Co/Rh$. A xenon (methane) proportional counter was used as a detector. Computer fits were performed to all measured spectra.

Preparations. $[Fe_2(H_2O)_2(BTC)_{4/3}]Cl\cdot 4.5(DMF)$ (**1**). The mixture of $FeCl_3$ (0.4 mmol, 0.065 g), H_3BTC (0.4 mmol, 0.082), $TEDA\cdot 6H_2O$ (0.6 mmol, 0.132 g), and DMF (12 mL) was sealed in a Teflon-lined autoclave and heated at 150 °C for 4 days, followed by slow cooling to room temperature. After being washed with DMF several times, **1** was collected as orange cubic crystals with a yield of about 75% (based on Fe). Elem Anal. Calcd: Fe, 14.17; C, 38.85; H, 5.05; N, 7.99. Found: Fe, 14.59; C, 37.98; H, 4.96; N, 7.13.

$[Fe_4Cl(BTC)_{8/3}]Cl_2\cdot H_2O\cdot 2.5(DEF)$ (**2**). The mixture of $FeCl_3$ (0.4 mmol, 0.065 g), H_3BTC (0.4 mmol, 0.082 g), $TEDA\cdot 6H_2O$ (0.6 mmol, 0.132 g), and DEF (10 mL) was sealed in a Teflon-lined autoclave and heated at 160 °C for 4 days. After cooling to room temperature, orange cubic crystals of **2** and a small quantity of bright yellow block crystals of $[Fe_2Cl_2(HBTC)_2]\cdot(HTEDA)_2$ (**3**) were obtained. The yield of **2** was about 50% (based on Fe). Samples of **2** for all measurements were picked out manually under an optical microscope. Compound **3** was only characterized by single-crystal X-ray diffraction and IR spectrum. Elem Anal. Calcd (%) for **2** : Fe, 19.38; C, 28.02; H, 3.28; N, 3.04. Found: Fe, 19.95; C, 27.59; H, 3.06; N, 2.82.

Ion-Exchange Experiment. An ion-exchange experiment was carried out for compound **1**: 1.46 g (15 mmol) of KCNS was dissolved in 50 mL of anhydrous ethanol in a vial, then a ca. 70 mg sample of **1** was added to the solution. The vial was covered, and the sample of **1** was soaked in the solution for 24 h. After being filtered and washed several times by anhydrous ethanol solvent, the ion-exchanged sample of **1** was collected for subsequent IR spectrum and X-ray powder diffraction (XRPD) studies.

Qualitative and Quantitive Experiments for Cl^- Anions. To confirm the existence of Cl^- anions in **1** and **2** qualitatively and determine their contents quantitively, the following experiments were carried out. Samples of **1** (124.11 mg) were dissolved in 40 mL of dilute HNO_3 solution (2 mol L^{-1}). After filtration, a $AgNO_3$ solution was added dropwise into the homogeneous filtrate and a white precipitate (AgCl) formed immediately. When no AgCl precipitate was formed any more, the mixture was filtered. After being washed several times by a dilute HNO_3 solution and deionized water, the AgCl precipitate was placed in a high-vacuum oven at 80 °C for 24 h. The dried AgCl weight was 21.44 mg, and the theoretical value according to the formula of **1** was 22.57 mg. A similar experiment was performed for **2** (82.46 mg) and 31.17 mg of AgCl (theoretical value: 30.75 mg) was obtained.

X-ray Crystallography. Diffraction intensities for compounds **1**−**3** were collected on a Siemens Smart CCD diffractometer with Mo Kα monochromatic radiation ($\lambda = 0.71073$ Å) at 293 K. The

(11) Brayshaw, S. K.; Green, J. C.; Hazari, N.; McIndoe, J. S.; Marken, F.; Raithby, P. R.; Weller, A. S. *Angew. Chem., Int. Ed.* **2006**, *45* (36), 6005−6008.
(12) Rowsell, J. L. C.; Yaghi, O. M. *Angew. Chem., Int. Ed.* **2005**, *44* (30), 4670−4679.
(13) Riou-Cavellec, M.; Albinet, C.; Grenèche, J. M.; Férey, G. *J. Mater. Chem.* **2001**, *11* (12), 3166−3171.
(14) Riou-Cavellec, M.; Férey, G. *Solid State Sci.* **2002**, *4* (9), 1221−1225.
(15) Sanselme, M.; Grenèche, J. M.; Riou-Cavellec, M.; Férey, G. *Chem. Commun.* **2002** (18), 2172−2173.
(16) Serre, C.; Millange, F.; Surblé, S.; Grenèche, J. M.; Férey, G. *Chem. Mater.* **2004**, *16* (14), 2706−2711.
(17) Sanselme, M.; Grenèche, J. M.; Riou-Cavellec, M.; Férey, G. *Solid State Sci.* **2004**, *6* (8), 853−858.
(18) Serre, C.; Millange, F.; Surblé, S.; Férey, G. *Angew. Chem., Int. Ed.* **2004**, *43* (46), 6286−6289.
(19) Sudik, A. C.; Cote, A. P.; Yaghi, O. M. *Inorg. Chem.* **2005**, *44* (9), 2998−3000.
(20) Sudik, A. C.; Millward, A. R.; Ockwig, N. W.; Cote, A. P.; Kim, J.; Yaghi, O. M. *J. Am. Chem. Soc.* **2005**, *127* (19), 7110−7118.
(21) Sudik, A. C.; Cote, A. P.; Wong-Foy, A. G.; O'Keeffe, M.; Yaghi, O. M. *Angew. Chem., Int. Ed.* **2006**, *45* (16), 2528−2533.
(22) Lii, K. H.; Huang, Y. F.; Zima, V.; Huang, C. Y.; Lin, H. M.; Jiang, Y. C.; Liao, F. L.; Wang, S. L. *Chem. Mater.* **1998**, *10* (10), 2599−2609.
(23) Zeng, M. H.; Feng, X. L.; Chen, X. M. *Dalton Trans.* **2004** (15), 2217−2223.
(24) Xie, L. H.; Liu, S. X.; Gao, B.; Zhang, C. D.; Sun, C. Y.; Li, D. H.; Su, Z. M. *Chem. Commun.* **2005** (18), 2402−2404.

Table 1. Crystal Data and Structure Refinement Results for **1**−**3**

	1	**2**	**3**
empirical formula	$C_{25.50}H_{39.50}ClFe_2N_{4.50}O_{14.50}$	$C_{36.50}H_{37.50}Cl_3Fe_4N_{2.50}O_{19.50}$	$C_{30}H_{34}ClFe_2N_4O_{12}$
M	788.27	1152.94	825.21
cryst syst	cubic	cubic	monoclinic
space group	$Fm\bar{3}m$	$Fm\bar{3}m$	$P2(1)/n$
a/Å	26.6328(4)	30.2083(16)	9.7827(4)
b/Å			18.9260(8)
c/Å			9.8318(4)
β/deg			116.2490(10)
V/Å^3	18890.8(5)	27566(3)	1632.62(12)
Z	24	24	2
ρ_{calc}/mg·m^{-3}	1.663	1.667	1.679
μ/mm^{-1}	1.084	1.491	1.123
reflns collected	24472	37205	8208
independent reflns	643	1100	2588
θ range/deg	1.32−25.00	1.17−25.50	2.15−25.00
GOF	1.052	1.045	1.061
R_1 [$I > 2\sigma(I)$][a]	0.0757	0.0577	0.0286
R_2(all data)[b]	0.2480	0.1711	0.0717

[a] $R_1 = \sum||F_o| - |F_c||/\sum|F_o|$. [b] $R_2 = [\sum w(F_o^2 - F_c^2)^2/\sum w(F_o^2)^2]^{1/2}$.

linear absorption coefficients, scattering factors for the atoms, and the anomalous dispersion corrections were taken from the International Tables for X-ray Crystallography. Empirical absorption corrections were applied. The structures were solved by the direct method and refined by the full-matrix least-squares method on F^2 using the *SHELXTL* crystallographic software package. All H atoms were placed geometrically for **1** and **2**, and partial H atoms (on the carboxyl group and protonated N atom of TEDA) were located from difference Fourier maps and refined isotropically for **3**. Anisotropic thermal parameters were used to refine all non-hydrogen atoms. In compound **2**, one type of BTC was disordered at two positions along the $\bar{3}$ axis, and thus C4 and O3 were set to be half-occupied. The frameworks of **1** and **2** were occupied by disordered guest molecules and Cl^- anions, which show many peaks of low electronic density in the difference Fourier maps. So the SQUEEZE subroutine of the *PLATON* software[25] was applied to create new reflection data where tje contributions from the disordered components are removed from the original data. Subsequent refinements were based on the new data. The number of disordered guest molecules and Cl^- ions was determined according to elemental analyses, TG analyses, qualitative and quantitive experiments for Cl^- anions, and charge balance. And these disordered components were all included in the final structure−factor calculations. The crystal data and structure refinement results of compounds **1**−**3** are summarized in Table 1.

Results and Discussion

Syntheses and Structures. Though the syntheses of **1** and **2** are not in strict nonaqueous conditions, the yields are sensitive to the amount of water in the systems. Even if the starting material of anhydrous ferric chloride ($FeCl_3$) was replaced by ferric chloride hexahydrate ($FeCl_3·6H_2O$), only a very small product amount was obtained, with much amorphous precipitation. Water molecules contained in the final products may derive from the deprotonation agent $TEDA·6H_2O$ or a little content of water in the solvents. In addition, Cl^- may also play an important role in the formation of **1** and **2**, because when $FeCl_3$ was replaced by $Fe_2(SO_4)_3$ or $Fe(NO_3)_3$, compounds **1** and **2** were not obtained. The modulation of the frameworks of **1** and **2** by different solvents reveals that there is mutual selectivity between the open frameworks and internal guests.

Compound **1**, $[Fe_2(H_2O)_2(BTC)_{4/3}]Cl·4.5(DMF)$, is a 3D framework constructed from paddlewheel Fe_2(II, III) units $[Fe_2(COO)_4(H_2O)_2]^+$ and triangular BTC linkers. The two crystallographically equivalent Fe atoms in a paddlewheel unit are five-coordinated with square-pyramidal geometry completed by four equatorial carboxyl O atoms and an axial water molecule. (Figure 2a) The lengths of the $Fe-O_{carboxyl}$ bonds are 2.048(4) Å, and the lengths of the $Fe-O_{aqua}$ bonds are 2.358(7) Å. In many mixed-valence trinuclear iron carboxylate complexes,[26−28] the $Fe^{III}-O_{carboxyl}$ distances are usually in the range of 2.02−2.04 Å and the $Fe^{II}-O_{carboxyl}$ distances are in the range of 2.10−2.12 Å. However, there are some differences between the trinuclear iron systems and the dinuclear iron unit herein; thus, we cannot determine the valences of the iron atoms in **1** only according to the Fe−O distances. Each paddlewheel unit in **1** is locked by four carboxyl groups from four equivalent BTC linkers, and each BTC linker connects three paddlewheel units, resulting in the 3D (3,4)-connected net with $Fm3m$ symmetry (Figure 2b). The topology of the framework can be regarded as the twisted boracite type with vertex symbols $6_2·6_2·8_2·8_2·12_2·12_2$ (for 4-connected vertex) and 6·6·6 (for 3-connected vertex). It is isomorphic with HKUST-1,[29] which is built from paddlewheel dicopper units and BTC. Paddlewheel dicopper and dizinc units have been extensively used as building blocks for the construction of metal−organic frameworks.[30−35] Chen and co-workers have reported that a metal−organic framework based on dicopper units exhibited increased

(25) Spek, A. L. *J. Appl. Crystallogr.* **2003**, *36*, 7−13.

(26) Sato, T.; Ambe, F.; Endo, K.; Katada, M.; Maeda, H.; Nakamoto, T.; Sano, H. *J. Am. Chem. Soc.* **1996**, *118* (14), 3450−3458.

(27) Wilson, C.; Iversen, B. B.; Overgaard, J.; Larsen, F. K.; Wu, G.; Palii, S. P.; Timco, G. A.; Gerbeleu, N. V. *J. Am. Chem. Soc.* **2000**, *122* (46), 11370−11379.

(28) Overgaard, J.; Larsen, F. K.; Schiott, B.; Iversen, B. B. *J. Am. Chem. Soc.* **2003**, *125* (36), 11088−11099.

(29) Chui, S. S. Y.; Lo, S. M. F.; Charmant, J. P. H.; Orpen, A. G.; Williams, I. D. *Science* **1999**, *283* (5405), 1148−1150.

(30) Chen, B. L.; Eddaoudi, M.; Hyde, S. T.; O'Keeffe, M.; Yaghi, O. M. *Science* **2001**, *291* (5506), 1021−1023.

(31) Eddaoudi, M.; Kim, J.; O'Keeffe, M.; Yaghi, O. M. *J. Am. Chem. Soc.* **2002**, *124* (3), 376−377.

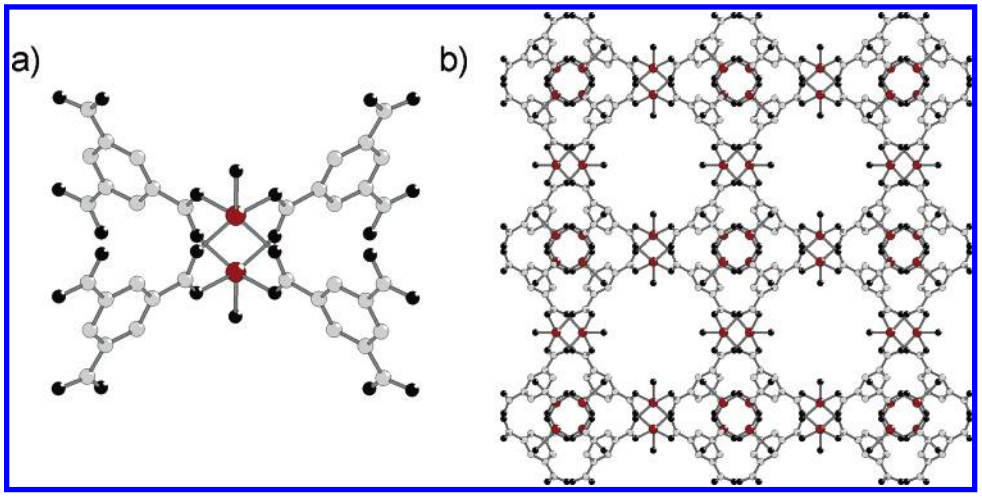

Figure 2. Perspective view of (a) the paddlewheel Fe_2 unit and (b) the (3,4)-connected framework of **1**. Dark red, black, and gray spheres represent Fe, O, and C atoms, respectively. Hydrogen atoms are not shown for clarity.

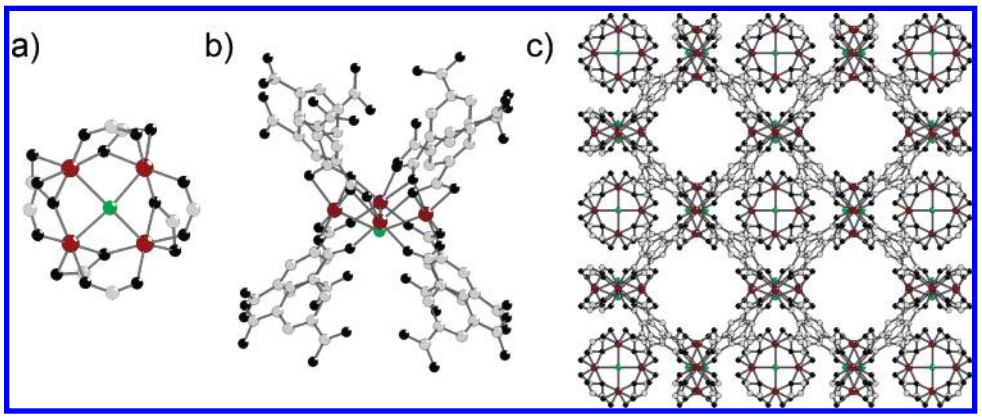

Figure 3. Perspective view of (a) the coordination geometries of the Fe atoms in (b) the square-planar Fe_4 unit and (c) the (3,8)-connected framework of **2**. Dark red, green, black, and gray spheres represent Fe, Cl, O, and C atoms, respectively. All hydrogen atoms are not shown for clarity.

hydrogen-storage capacity when open metal sites were achieved by removing the axial water ligands.[36] The paddlewheel diiron unit, however, has not been observed in metal−organic frameworks, although similar discrete units have been reported in some works about modeling non-heme diiron enzymes, which are obtained with the utilization of sterically hindered carboxylate ligands.[37−40] The Mössbauer spectrum study (vide infra) for **1** illustrates that the two iron atoms in a Fe_2 unit are divalent and trivalent, respectively. Consequently, the overall framework is cationic, and a Cl^- anion per formula ought to be inside the framework for charge balance. Indeed, the existence of one Cl^- ion per formula in **1** was confirmed by the experiments for determining Cl^- (see the Experimental Section) and the XPS of compound **1** (see the Supporting Information, Figure S3). Besides the Cl^- ion, approximately 4.5 additional DMF molecules per formula reside inside the framework, which is determined based upon the TG curve and elemental analyses of **1**. The total volume occupied by the disordered components is estimated to be 11897.00 $Å^3$ per unit cell.[25]

Compound **2**, $[Fe_4Cl(BTC)_{8/3}]Cl_2 \cdot H_2O \cdot 2.5(DEF)$, crystallizes in the identical space group ($Fm\bar{3}m$) of **1**. It is a 3D framework constructed from tetrameric square-planar Fe_4(III, III, III, II) units $[Fe_4Cl(COO)_8]^{2+}$ and BTC linkers. The four Fe atoms in each Fe_4 unit are crystallographically equivalent, and each Fe center is six-coordinated with distorted-octahedron geometry, which is completed by five carboxyl O atoms from four BTC units and a μ_4-Cl atom with the $Fe-O_{carboxyl}$ distances ranging from 2.038(2) to 2.190(2) Å and the Fe−Cl distance being 2.454(2) Å (Figure 3a). Eight carboxyl groups from eight BTC linkers ligate the four iron atoms in square geometry supported with a Cl atom in the middle (Figure 3b). There are two types of BTC linkers in **2**. The carboxyl groups of one type coordinate Fe atoms in dimonodentate fashion and for the other type in the chelate-bridging mode fashion. However, both types of

(32) Eddaoudi, M.; Kim, J.; Vodak, D.; Sudik, A.; Wachter, J.; O'Keeffe, M.; Yaghi, O. M. *Proc. Natl. Acad. Sci. U.S.A.* **2002**, *99* (8), 4900−4904.
(33) Dybtsev, D. N.; Chun, H.; Kim, K. *Angew. Chem., Int. Ed.* **2004**, *43* (38), 5033−5036.
(34) Chun, H.; Dybtsev, D. N.; Kim, H.; Kim, K. *Chem.—Eur. J.* **2005**, *11* (12), 3521−3529.
(35) Wang, Z. Q.; Kravtsov, V. C.; Zaworotko, M. J. *Angew. Chem., Int. Ed.* **2005**, *44* (19), 2877−2880.
(36) Chen, B. L.; Ockwig, N. W.; Millward, A. R.; Contreras, D. S.; Yaghi, O. M. *Angew. Chem., Int. Ed.* **2005**, *44* (30), 4745−4749.
(37) Yoon, S. H.; Lippard, S. J. *Inorg. Chem.* **2003**, *42* (26), 8606−8608.
(38) Hilderbrand, S. A.; Lippard, S. J. *Inorg. Chem.* **2004**, *43* (17), 5294−5301.
(39) Yoon, S.; Lippard, S. J. *J. Am. Chem. Soc.* **2005**, *127* (23), 8386−8397.
(40) Chavez, F. A.; Ho, R. Y. N.; Pink, M.; Young, V. G.; Kryatov, S. V.; Rybak-Akimova, E. V.; Andres, H.; Munck, E.; Que, L.; Tolman, W. B. *Angew. Chem., Int. Ed.* **2002**, *41* (1), 149−152.

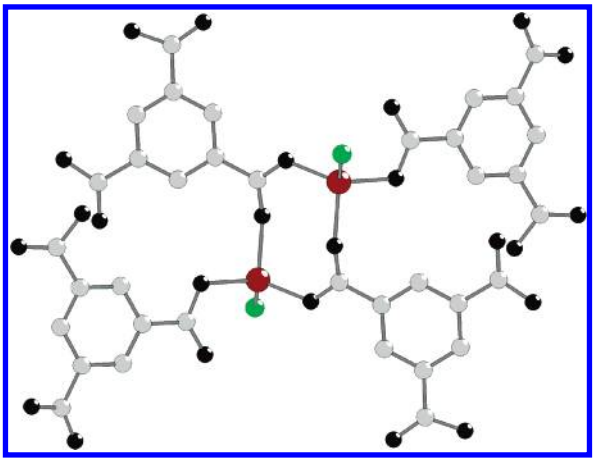

Figure 4. Perspective view of the Fe_2 unit in **3**. Dark red, green, black, and gray spheres represent Fe, Cl, O, and C atoms, respectively. Hydrogen atoms are not shown for clarity.

BTC linker connect three Fe_4 units. The propagation of the square-planar and triangular units forms the (3,8)-connected network of **2** (Figure 3c). Recently, Ma and Zhou have reported a porous metal−organic framework with two interpenetrated (3,8)-connected networks built from square-planar Co_4 and triangular TATB (4,4′,4″-*s*-triazine-2,4,6-triyltribenzoate) units.[41] To our knowledge, that is the first (3,8)-connected net observed. Theretofore, only a hypothetical (3,8)-connected net had been put forward.[42] The vertex symbols of the (3,8)-connected net are $4{\cdot}4{\cdot}4{\cdot}4{\cdot}4{\cdot}4{\cdot}4{\cdot}4{\cdot}6_2{\cdot}6_2{\cdot}6_2{\cdot}6_2{\cdot}8_4{\cdot}8_4{\cdot}8_4{\cdot}8_4{\cdot}8_8{\cdot}8_4{\cdot}8_8{\cdot}8_8{\cdot}8_4{\cdot}8_4{\cdot}8_4{\cdot}8_4{\cdot}8_8{\cdot}12_{32}{\cdot}12_{32}{\cdot}12_{32}{\cdot}12_{32}$ (for the 8-connected vertex) and $4{\cdot}4{\cdot}4$ (for the 3-connected vertex). The Mössbauer spectrum study for **2** (vide infra) reveals that three iron atoms are trivalent and that the other one is divalent in each Fe_4 unit. Similar to compound **1**, diffuse Cl^- anions and guest DEF molecules inside the framework could not be modeled in crystallographic study. The total volume occupied by the disordered components is 10039.00 Å^3 per unit cell.

Compound **3**, $[Fe_2Cl_2(HBTC)_2]{\cdot}(HTEDA)_2$, consists of two-dimensional metal−organic layers and protonated TEDA molecules between the adjacent layers. The layer is constructed from dimeric Fe_2 units and BTC linkers. Each equivalent Fe atom in the Fe_2 unit is coordinated with three carboxyl O atoms from three BTC units and a Cl atom with distorted-tetrahedron geometry (Figure 4). Each BTC linker in **3** links two Fe_2 units with its two carboxyl groups in dimonodentate and monodentate fashions, respectively. The third carboxyl group is protonated and pointing to the interlamellar space. Each Fe_2 unit is connected to four neighboring Fe_2 units by four BTC linkers, resulting in the two-dimensional layer along the *ab* plane (see the Supporting Information, Figure S14). Protonated TEDA molecules reside between the adjacent layers stabilized by hydrogen-bonding interactions between carboxyl O atoms, Cl atoms on the layers, and N atoms of TEDA (Table 2 and Supporting Information, Figure S15). According to the structure determination, all the Fe atoms should be divalent according to charge balance.

Table 2. Hydrogen-Bond Geometry for **3**

D−H···A	D−H (Å)	H···A (Å)	D···A (Å)	D−H···A (deg)
N2−H4···O2[a]	0.84(3)	2.22(2)	2.893(2)	136
N2−H4···Cl1[a]	0.84(3)	2.69(3)	3.333(2)	134(2)
O6−H17···N1[b]	0.81(4)	1.84(4)	2.627(2)	165(4)

[a] Symmetry code: $x - 1/2, -y + 1/2, z + 1/2$. [b] Symmetry code: $x + 1, y, z + 1$.

Table 3. Parameters of Least-Squares-Fitted Mössbauer Spectroscopy for **1** and **2**[a]

	doublet	δ	ΔE_Q	$\Gamma/2$	area ratio (%)
1	a	0.41(1)	0.78(2)	0.26(1)	49.3
	b	1.08(1)	1.66(3)	0.41(1)	50.7
2	a	0.43(1)	0.85(1)	0.30(1)	78.4
	b	1.02(1)	1.81(3)	0.37(2)	21.6

[a] Abbreviations: δ = isomer shift referred to α-Fe foil (mm s^{-1}); ΔE_Q = quadrupole splitting (mm s^{-1}); $\Gamma/2$ = half-width of the lines (mm s^{-1}).

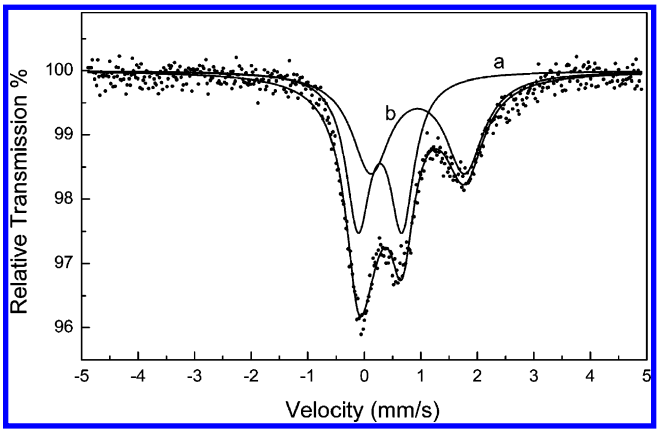

Figure 5. Mössbauer spectrum of **1** recorded at 293 K.

Mössbauer Spectroscopy. To determine the valences of the Fe atoms in **1** and **2**, the studies of Mössbauer spectra for the compounds were carried out at ambient temperature. For **1**, the Mössbauer spectrum consists of two quadrupole-split doublets (Figure 5), the parameters of which were obtained by least-squares fitting and are listed in Table 3. The doublet with isomer shift value $\delta = 0.41$ mm s^{-1} and quadrupole-splitting value $\Delta E_Q = 0.78$ mm s^{-1} is typical of high-spin trivalent iron atoms,[43,44] and the other with $\delta = 1.08$ mm s^{-1} and $\Delta E_Q = 1.66$ mm s^{-1} corresponds to high-spin divalent iron atoms.[13,44] The area ratio for the two doublets is about 51:49. These results illustrate that there are Fe(II) and Fe(III) atoms in **1** with a 1:1 quantitive ratio. According to the structure of **1**, it is reasonable to assign one Fe(II) cation and one Fe(III) cation to each paddlewheel Fe_2 unit.

The Mössbauer spectrum for **2** can be fitted into two quadrupole-split doublets, as well (Figure 6). They can be assigned to one type of high-spin trivalent iron ($\delta = 0.43$

(41) Ma, S.; Zhou, H. C. *J. Am. Chem. Soc.* **2006**, *128* (36), 11734−11735.
(42) Bucknum, M. J.; Castro, E. A. *Cent. Eur. J. Chem.* **2005**, *3* (1), 169−173.
(43) Bino, A.; Shweky, I.; Cohen, S.; Bauminger, E. R.; Lippard, S. J. *Inorg. Chem.* **1998**, *37* (20), 5168−5172.
(44) Overgaard, J.; Rentschler, E.; Timco, G. A.; Gerbeleu, N. V.; Arion, V.; Bousseksou, A.; Tuchagues, J. P.; Larsen, F. K. *J. Chem. Soc., Dalton Trans.* **2002** (*15*), 2981−2986.

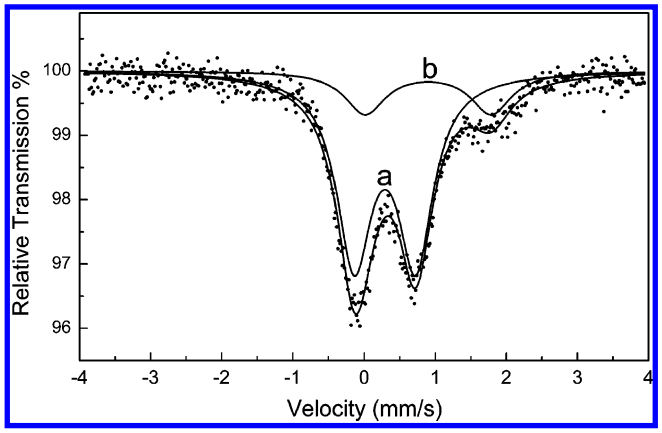

Figure 6. Mössbauer spectrum of **2** recorded at 293 K.

mm s^{-1}, ΔE_Q = 0.85 mm s^{-1}) and one type of high-spin divalent iron (δ = 1.02 mm s^{-1}, ΔE_Q = 1.81 mm s^{-1}). The area ratio of the two doublets is about 78:22 (Fe(III)/Fe(II)). With consideration of the structure of **2**, we presume that the Fe(III)/Fe(II) ratio should be 3:1 (three Fe(III) and one Fe(II) in each Fe_4 unit) in **2**.

The results of the Mössbauer spectra studies reveal that the Fe atoms in **1** and **2** are in two distinct valence states. Due to the crystallographically imposed symmetry ($m\bar{3}$ m), Fe atoms with different valences in **1** or **2** are crystallographically equivalent. A similar situation has also been found in some high-symmetry mixed-valence trinuclear iron carboxylate complexes.[45−47] Generally, it is supposed that the similar coordination geometries of the Fe atoms with different valences in mixed-valence systems mainly derive from disorder, either static or dynamic, or electron delocalization.[27] However, the valence states of the Fe atoms in **1** and **2** can be trapped in the Mössbauer spectrum, indicating that the rates of electron transfer in **1** and **2** are less than the Mössbauer time scale (10^6−10^7 s^{-1}) at 293 K.[46]

Magnetic Properties. Magnetic studies have been performed on powdered samples for **1** and **2** in the range of 2−300 K. For **1**, the product $\chi_m T$, where χ_m is the molar magnetic susceptibility in terms of the formula, decreases gradually from 300 to 2 K, indicating the presence of antiferromagnetic exchange interactions in **1** (Figure 7). The absence of a maximum on the susceptibility versus temperature curve indicates that the antiferromagnetic interactions are weak and long-range order has still not been achieved at 2 K. The magnetic data obey the Curie−Weiss law throughout the temperature range. The linear fitting of the reciprocal of the susceptibility versus temperature plot gives values of C = 7.84 cm^3 mol^{-1} K and θ = −9.32 K. These results are in agreement with the structure character of **1**, where Fe_2 units are separated far from each other by BTC linkers. The $\chi_m T$ value at room temperature (7.60 cm^3 mol^{-1} K) is close

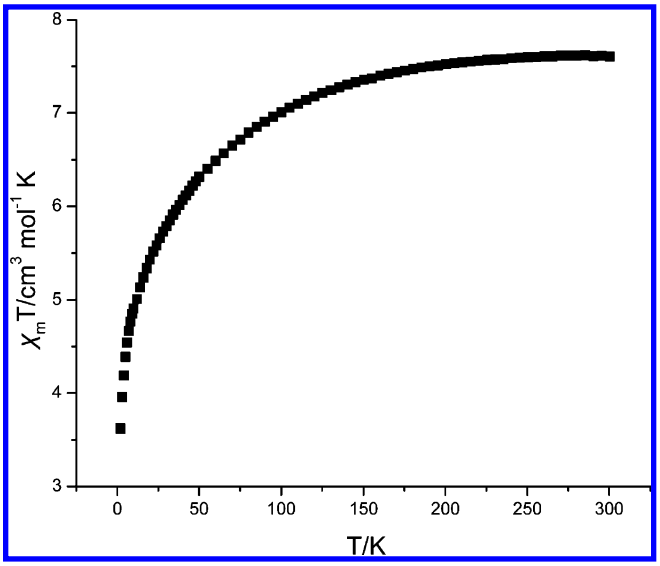

Figure 7. Plot of $\chi_m T$ versus T for compound **1**.

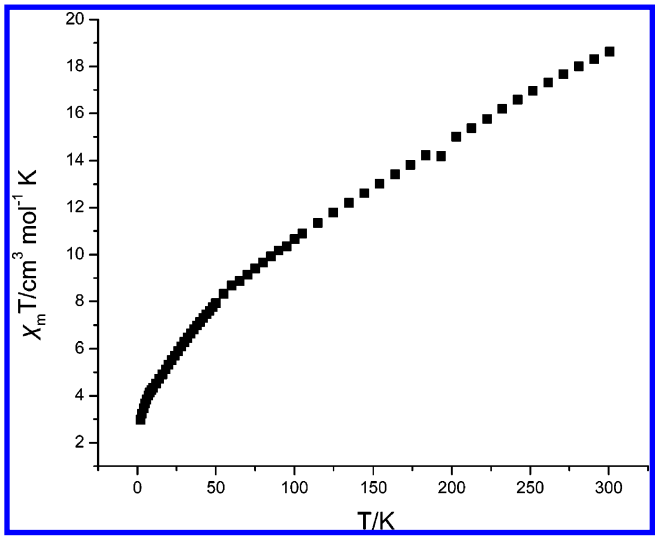

Figure 8. Plot of $\chi_m T$ versus T for compound **2**.

to the expected value (7.38 cm^3 mol^{-1} K, assuming g = 2.0 for Fe^{2+} and Fe^{3+}) for one high-spin Fe(III) atom and one high-spin Fe(II) atom in each paddlewheel Fe2 unit per formula. This accordance also justifies the assignment of the valences of the iron atoms in **1**.

The magnetic property of **2** is similar to that of **1**. From 300 to 2 K, the $\chi_m T$ value decreases steadily, revealing the presence of antiferromagnetic exchange interactions (Figure 8). The magnetic data only obey the Curie−Weiss law in the high-temperature region, indicating that the antiferromagnetic interactions are stronger than those in **1**. Linear fitting of the reciprocal of susceptibility versus temperature curve with the Curie−Weiss law in the range of 150−300 K gives values of C = 35.45 cm^3 mol^{-1} K and θ = −274.31 K. The $\chi_m T$ value at room temperature (18.63 cm^3 mol^{-1} K) is slightly higher than the expected value (16.13 cm^3 mol^{-1} K, assuming g = 2.0 for Fe^{2+} and Fe^{3+}) for three high-spin Fe(III) atoms and one high-spin Fe(II) atom in each Fe_4 unit per formula.

Host−Guest Studies. Since there are large volumes inside the framework of **1** and **2** occupied by Cl^- ions and guest

(45) Woehler, S. E.; Wittebort, R. J.; Oh, S. M.; Hendrickson, D. N.; Inniss, D.; Strouse, C. E. *J. Am. Chem. Soc.* **1986**, *108* (11), 2938−2946.
(46) Woehler, S. E.; Wittebort, R. J.; Oh, S. M.; Kambara, T.; Hendrickson, D. N.; Inniss, D.; Strouse, C. E. *J. Am. Chem. Soc.* **1987**, *109* (4), 1063−1072.
(47) Jang, H. G.; Geib, S. J.; Kaneko, Y.; Nakano, M.; Sorai, M.; Rheingold, A. L.; Montez, B.; Hendrickson, D. N. *J. Am. Chem. Soc.* **1989**, *111* (1), 173−186.

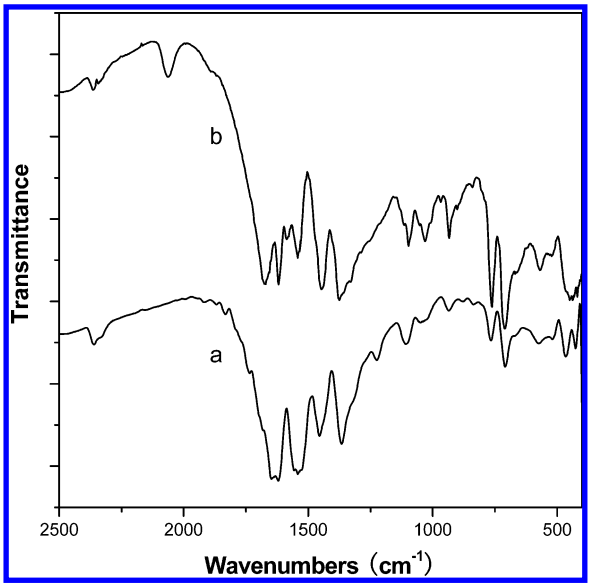

Figure 9. IR spectra of the as-synthesized (a) and ion-exchanged (b) samples of **1** shown in the range of 1000−2500 cm^{-1}.

molecules, we have investigated the host−guest properties of the compounds. Initially, we attempted to remove the guests by heating with the frameworks retained; however, this attempt failed. The resultant samples after heating are amorphous according to their XRPD patterns. It may be that the interactions between the guests, Cl^- ions, and host frameworks are fairly strong, so the frameworks were broken down via direct heating. Subsequently, we carried out an ion-exchange experiment for compound **1**, the details of which are described in the Experimental Section. After the as-synthesized sample of **1** was soaked in an anhydrous ethanol solution of KCNS for 24 h, the ion-exchanged sample was obtained. In the IR spectra of the ion-exchanged sample of **1**, compared to that of the as-synthesized sample, a new band at 2065 cm^{-1} appears, and the profiles of other bands are essentially unchanged but only with slight shifts to the higher or lower wavenumbers (Figure 9). The new band at 2065 cm^{-1} corresponds to the characteristic stretching vibration of the C≡N bond of the CNS^- anion.[48,49] These results unambiguously indicate that the Cl^- anions in the as-synthesized sample of **1** have been exchanged by CNS^- anions in the solution. The slight shift of the other bands may exist because the components of **1** had been slightly affected when Cl^- was exchanged by CNS^- anions. Furthermore, the XRPD pattern of the ion-exchanged sample shows that the crystalline state of the framework of **1** is retained after ion exchange (Figure 10).

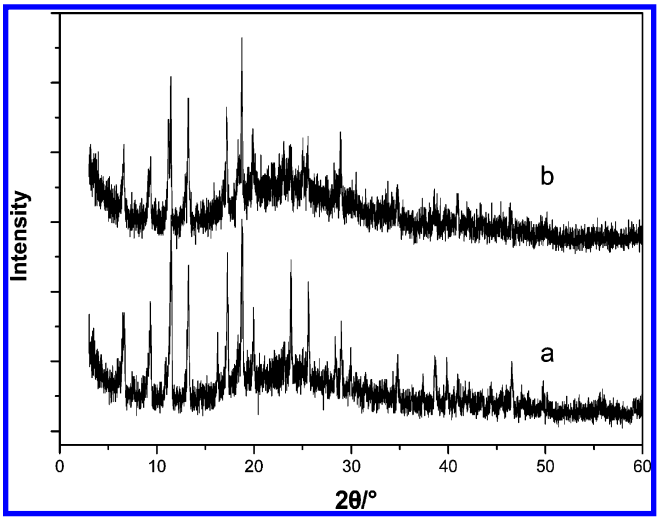

Figure 10. XRPD patterns for as-synthesized (a) and ion-exchanged (b) samples of **1**.

Conclusion

The syntheses and structure investigations of **1** and **2** provide us some insight about the formation of iron−organic frameworks. The valences of iron atoms are changeable in solvothermal conditions; thus, the frameworks can be readily affected by solvents (or possibly some other factors) in the process of crystallization. This character may allow modulations of iron−organic frameworks to obtain porous materials with walls containing electron-active sites and special sized and shaped pores, which are of great importance in many potential applications, such as gas storage and catalysis. However, the reaction mechanism is elusive because there may be many factors that can influence the structures of the frameworks and especially the complex redox reactions that would take place around the Fe cations. We are now going on with our investigation of the system and expect that more results will be obtained in the future.

Acknowledgment. This work was supported by the National Science Foundation of China (Grant No. 20571014), the Scientific Research Foundation for Returned Overseas Chinese Scholars, the Ministry of Education, and the Analysis and Testing Foundation of Northeast Normal University. We thank Prof. Milan Liu (Jilin University) for her assistance on the measurements and discussions of the Mössbauer spectra.

Supporting Information Available: Crystallographic data of **1**−**3** in CIF format; TG curves, XRPD patterns, XPS, IR spectra, and additional figures relative to the compounds in PDF format. This material is available free of charge via the Internet at http://pubs.acs.org.

IC062273M

(48) Fang, Q. R.; Zhu, G. S.; Xue, M.; Sun, J. Y.; Wei, Y.; Qiu, S. L.; Xu, R. R. *Angew. Chem., Int. Ed.* **2005**, *44* (25), 3845−3848.
(49) Zhang, X. M.; Fang, R. Q.; Wu, H. S. *J. Am. Chem. Soc.* **2005**, *127* (21), 7670−7671.